Failure Assessment of Pipeline Anti-corrosion Coating Based on Monte Carlo and Improved BPNN

Jing Wang, Hongyu Gu*, Hongyan Fu, Songlin Li

Abstract—The anti-corrosion coating of pipeline systems, as a key infrastructure in cities and industries, is affected by various environmental factors during long-term use, resulting in pipeline corrosion and safety hazards. To improve the accuracy and reliability of failure assessment of pipeline anti-corrosion coatings, this study proposes a backpropagation neural network framework that integrates Monte Carlo simulation and improved particle swarm optimization. This framework generates a dataset covering multidimensional random parameters, such as corrosion depth and pipe diameter, through the Monte Carlo method, quantifying the nonlinear evolution law of corrosion. The dynamic inertia weight and genetic crossover operator optimization particle swarm algorithm are designed to enhance the global search ability and classification accuracy of the neural network. The experiment showed that the Monte Carlo simulation reduced the error to 0.5% after 106 iterations, and the prediction error of deep corrosion failure probability was only 0.47%. The improved model achieved a precision of 97.2% and a recall of 97.1% on the test set, which was 12.2% higher than the traditional backpropagation neural network. The risk level classification correlation coefficient R was greater than 0.99. This framework enhances the accuracy and classification reliability of pipeline failure risk assessment through data-driven and intelligent optimization collaboration, providing technical support for the full lifecycle safety management of corroded pipelines.

Keywords—Monte Carlo; Pipeline corrosion; BPNN; Grade classification

I. INTRODUCTION

The pipeline network system is a key infrastructure for modern cities and industrial production, and its safe operation is related to energy transmission, water supply stability, and production continuity. However, under long-term service, the Anti-corrosion Coating of the Pipeline

Manuscript received June 5, 2025; revised August 20, 2025.

The work was supported by 2024 Hebei Zhongyan Industry Co., Ltd. Technology Project: "Corrosion Analysis and Water Treatment Protection Study of Softened Water in Factory Hot Water Pipeline Network" (HBZY-BY2024A006).

Jing Wang is a senior engineer of Baoding Cigarette Factory of Hebei Baisha Tobacco Co., Ltd., Baoding 071000, China (e-mail: bdwj881111@126.com).

Hongyu Gu is an engineer of Baoding Cigarette Factory of Hebei Baisha Tobacco Co., Ltd., Baoding 071000, China (corresponding author to provide e-mail: sjs091240@outlook.com).

Hongyan Fu is an engineer of Baoding Cigarette Factory of Hebei Baisha Tobacco Co., Ltd., Baoding 071000, China (e-mail: xyh8794@126.com).

Songlin Li is an engineer of Baoding Cigarette Factory of Hebei Baisha Tobacco Co., Ltd., Baoding 071000, China (e-mail: dl0110dl@outlook.com).

Network (ACCPN) is susceptible to performance degradation and failure due to the coupling effects of multiple factors such as soil chemical properties, microbial activity, stray currents, and fluctuations in operating conditions, leading to corrosion and perforation of the pipeline body. Even more, it can lead to serious consequences such as environmental pollution, production interruptions, and secondary disasters. Therefore, accurately and efficiently assessing the risk of ACCPN failure is of crucial practical significance for developing preventive maintenance strategies, optimizing asset lifecycle management, and ensuring the safe operation of infrastructure [1]. The traditional ACCPN failure assessment method mainly relies on empirical formulas, deterministic models, and on-site detection data. Although these methods can provide preliminary diagnosis, they often expose shortcomings such as insufficient accuracy and weak generalization ability when facing multi-parameter uncertainty, nonlinear evolution, time-varying characteristics of corrosion processes under complex working conditions [2]. The Monte Carlo method, as a numerical simulation technique based on probability statistics, can quantify the spatiotemporal evolution of pipeline failure probability by constructing a random distribution model of input parameters and combining a large number of repeated sampling and simulation calculations [3]. Back Propagation Neural Network (BPNN) constructs a functional relationship from input parameters to output results by simulating the nonlinear mapping mechanism of human brain neurons. After training with historical data, the model can quickly classify the failure risk level of pipelines based on real-time detection of corrosion defect length, depth, and other features [4]. To achieve an accurate assessment of ACCPN failure state, this study uses Monte Carlo Simulation (MCS) to generate a dataset covering multidimensional random parameters, quantifying the nonlinear effects of corrosion kinetics. A BPNN model based on dynamic weight optimization is designed to achieve intelligent classification of failure risk levels.

The innovation of the research lies in proposing a BPNN framework that integrates an improved MCS and Particle Swarm Optimization (PSO) algorithm for ACCPN failure assessment. By introducing a power-law model to describe the nonlinear time-varying characteristics of corrosion depth, and using nonlinear inertia weights and genetic crossover operators to optimize PSO, the global search capability of BPNN is enhanced. The contribution lies in the construction of a high-precision and highly robust comprehensive evaluation system, which provides a reference basis for the full lifecycle risk assessment of ACCPN.

II. RELATED WORKS

In recent years, the corrosion failure assessment of pipeline systems has gradually integrated stochastic modeling and data-driven methods. MCS has become a core tool for reliability analysis due to its high tolerance for parameter uncertainty. Hou et al. proposed a framework based on MCS to evaluate the reliability of pipeline networks under earthquakes, taking into account spatial parameters such as peak ground velocity and pipe wall thickness. The redundancy of pipeline network topology would affect the evaluation of spatial correlation on connectivity reliability, and networks with high redundancy would overestimate reliability by ignoring spatial correlation [5]. Lin et al. used MCS of random corrosion distribution and Euler beam theory to construct a pipe soil interaction model for studying the effect of pitting corrosion on the buckling of submarine pipelines. Different corrosion distribution patterns, even with the same parameters, could lead to differentiated buckling displacement and strength attenuation [6]. Zhao et al. proposed a source term estimation method based on an improved Gaussian plume model and UAV laser methane sensing for natural gas pipeline leak detection. This method could synchronously locate the location and rate of leakage. Simulation verification showed that its accuracy was affected by the forward model and data reliability, and the inversion accuracy could be improved through prior information optimization [7]. Proenca et al. proposed an analytical model based on compressed wave and Rayleigh wave paths to simplify the location of water network leaks, and combined it with MCS parameter uncertainty analysis. Parameterized research showed that the maximum error of dual wave joint positioning was 15 cm, which improved the accuracy by 27.4% compared to a single wave path [8].

BPNN utilizes its powerful nonlinear mapping and self-learning capabilities to predict and evaluate pipeline states. Wu et al. proposed a hybrid model built on improved WOA and BPNN to improve the accuracy of pipeline damage identification. The model was optimized through a adaptive coefficients and random optimal replacement strategy. This model had a relative error of less than 2.2% in locating and predicting the degree of damage to fixed pipelines at both ends, and its overall performance was better than the comparative model [9]. Yin et al. designed a cold finger experiment to analyze the effects of temperature, shear force, and other parameters on diesel wax deposition pollution during sequential transportation of finished oil pipelines in cold regions. The BPNN prediction of deposition rate was optimized using the bald eagle search algorithm. The sedimentation rate increased with the increase of oil temperature and wax content, and the accuracy and generalization ability were effectively verified [10]. Sun et al. conducted experiments to accurately predict the roughness coefficient of sediment containing drainage pipes by measuring parameter changes under different sediment thicknesses, flow rates, and slopes, and optimized BPNN using genetic algorithms. BPNN and the improved model have increased the coefficient of determination by 3.47% and 3.99% compared to the traditional formula, and reduced the MAE by 41.18% and 47.06% [11]. Xiao et al. predicted the liquid holdup of wet gas pipelines and used grey relational analysis to screen seven input parameters, including pipe diameter and inclination angle, to construct a tuna swarm algorithm to optimize the BPNN model. The average absolute percentage errors of upward, downward, and horizontal pipelines were 5.32%, 10.19%, and 4.80%, with R² exceeding 0.99 [12].

In summary, existing Monte Carlo methods mostly focus on a single corrosion model, such as linear or static distribution, and fail to fully consider the nonlinear changes in corrosion rate over time and multi-parameter coupling effects, resulting in significant long-term prediction bias. In addition, BPNN relies on the traditional gradient descent method, which is prone to getting stuck in local optimal solutions due to the influence of initial weights, especially for predicting high-risk samples with insufficient accuracy. Therefore, this study proposes an evaluation framework that integrates MCS and PSO-BPNN. This framework accurately describes the nonlinear growth of corrosion depth through a power law model. At the same time, it introduces a PSO algorithm with nonlinear inertia weights and genetic crossover operators to optimize BPNN, improve the model's generalization performance, and ultimately achieve accurate classification of corrosion failure risk.

III. METHODS AND MATERIALS

A. Simulation of failure probability distribution of anti corrosion coating based on Monte Carlo method

ACCPN failure assessment needs to take into account both parameter uncertainty and corrosion dynamic evolution characteristics. Traditional deterministic methods can easily lead to prediction bias due to neglecting statistical distribution and temporal dependence. Therefore, this study constructs a failure probability simulation framework based on the Monte Carlo method. The basic idea of MCS is to use random numbers to simulate the input variables of a system, and calculate the system's output based on the values of these input variables. By repeating this process extensively, the distribution of output results can be obtained. For the failure assessment of ACCPN, the failure probability *P* calculated based on Monte Carlo is shown in equation (1) [13].

$$p = \lim_{n \to \infty} P\{h(A_1, A_2, \dots, A_n) \le A_n\} = F / E$$
 (1)

In equation (1), $h(\cdot)$ is the predictive model for the critical pressure of pipe rupture. (A_1,A_2,\cdots,A_n) is a sample dataset generated through independent random sampling that conforms to the statistical characteristics of the failure variable. F and E are the number of data and the total number of sample data that are less than or equal to the safety threshold. $P\{\cdot\}$ is the probability of event $h(\cdot)$ occurring. As the sample size approaches infinity, Monte Carlo accurately estimates this probability value through a large number of random simulations [14]. The probability prediction process of Monte Carlo method is shown in Figure 1.

In Figure 1, when using the Monte Carlo method to predict the probability of pipeline failure, the Pipeline Failure Pressure (PEP) is used as the target variable, and related parameters such as pipe diameter and corrosion depth are determined. Afterwards, based on historical data

engineering experience, reasonable probability distributions are set for these parameters, and the total number of simulations is determined. Subsequently, it enters the loop simulation phase, randomly selecting a set of data from the probability distribution of each parameter and substituting it into the critical state function for pipeline rupture failure calculation to determine whether the pipeline has failed. When the number of simulations reaches the preset total, the failure probability of the pipeline is calculated by the ratio of the number of failures to the total number of simulations. Due to the fact that the target variable in MCS is the critical pressure for pipe rupture, i.e., the failure pressure, this study mainly focuses on the failure risk assessment of this pressure. This study uses the Norwegian Classification Society standard F101 to solve and predict the PEP networks. The mathematical model of this standard is shown in equation (2) [15].

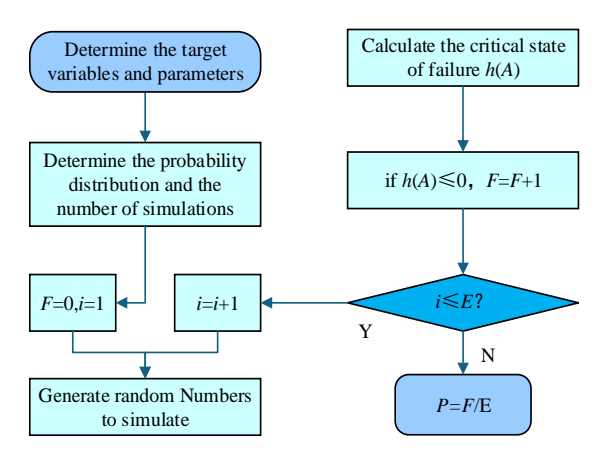


Figure 1 Monte Carlo probability prediction process of the method

$$\begin{cases} F_p = \upsilon \frac{2t}{D - t} \left[\frac{1 - \frac{d(T)}{t}}{1 - \frac{d(T)}{tQ}} \right] \\ Q = \sqrt{1 + 0.31 \frac{L(T)^2}{Dt}} \end{cases}$$
 (2)

In equation (2), F_p represents the PEP. t and T are the pipe wall thickness and pipe service life. L(T) denotes a function of the relationship between corrosion length and time. D is the pipe diameter, v is the ultimate tensile strength, d(T) is a function of the relationship between corrosion depth and time, and Q is the coefficient of expansion. In this model, the failure pressure has significant time-dependent characteristics, so the randomness of corrosion parameters can be ignored in probabilistic reliability assessment, and conservative evaluation results can be predicted based on corrosion defects. Although cathodic protection, organic coatings, and other protective measures are commonly used in engineering to slow down the corrosion process, the corrosion inhibition effect of such protective measures will significantly weaken in areas where macroscopic defects have already formed in the pipe body. Therefore, reasonable simplification should be made in the modeling of corrosion evolution [16]. The depth variation of corrosion defects on the pipe wall follows a power function

constitutive relationship, as shown in equation (3).

$$\begin{cases} d(T) = \lambda (T - T_1)^{\gamma} \\ L(T) = L_{\gamma} + \frac{L_{\gamma} (T - T_2)}{\Delta T} \end{cases}$$
 (3)

In equation (3), T_1 and T_2 are the times when the pipeline experiences longitudinal and transverse corrosion. L_i is the initial length of the corrosion defect. λ and γ are corrosion growth coefficients, which are determined based on historical data and characterize the variation of corrosion depth over time. ΔT is the detection time interval. To make the predicted PEP closer to the actual situation, this study introduces a variable error between the actual value and the predicted value of the failure pressure, and corrects the failure pressure obtained from MCS. The corrected failure pressure F_p' is shown in equation (4).

$$F_p' = F_r + M(0, \sigma^2) + \eta \tag{4}$$

In equation (4), F_r is the predicted value of failure pressure. M represents a variable with a variance of σ^2 , a mean of 0, and follows a normal distribution, while η is the average error of failure pressure prediction. The probability of pipeline failure is determined by the actual values of pipeline working pressure and PEP. The condition for pipeline rupture and failure is when the PEP is lower than the working pressure inside the pipeline. This study defines the critical state as equation (5).

$$\begin{cases} h(A) = F_p - P_w \\ P_w = \frac{2t}{D} \varepsilon \times S_f \times X_f \times Y_f \times Z_f \end{cases}$$
 (5)

In equation (5), P_w is the working pressure inside the pipeline. \mathcal{E} is the yield strength of the material. X_f , Y_f , and Z_f are temperature, joint, and line coefficients, all with values of 1. S_f is the safety factor, taken as 0.8. According to the statistical characteristics of pipeline corrosion failure cases and structural reliability theory, the probability of pipeline failure can be simulated by comparing the pipeline working pressure and PEP [17]. The probability classification of pipeline failure risk is shown in Figure 2.

In Figure 2, the probability of pipeline failure is divided into four risk levels. When the failure probability ranges from 0% to 25%, 25% to 50%, 50% to 75%, and 75% to 100%, the failure risk levels are low, medium, high, and extremely high, respectively. After determining the risk probability distribution, it is necessary to determine the variable data for MCS. This study is based on the engineering experience data range of pipeline geometric features and material properties, combined with the key parameters required for the fracture pressure prediction model. A sample dataset covering key parameters such as pipe diameter size, pipe wall thickness, operating time, and material strength is randomly generated for MCS. Table 1 shows the types of pipeline distribution and variable

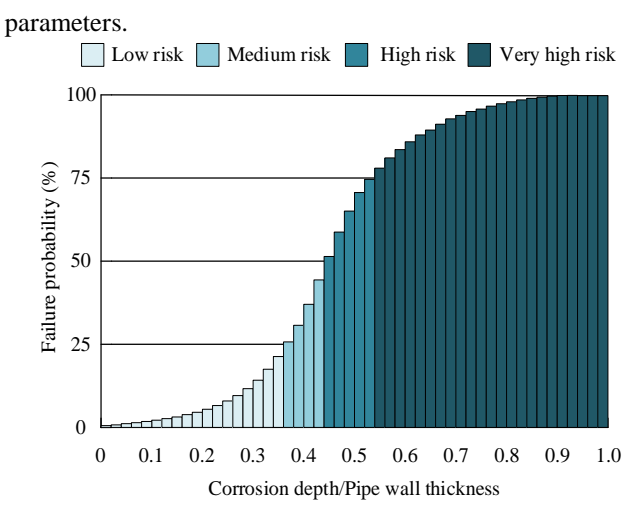


Figure 2 Pipeline failure risk level

TABLE 1
PIPELINE VARIABLE PARAMETERS AND DISTRIBUTION TYPES

Pipeline variable	Distribution type	Standard deviation	Mean value
Yield strength ε/MPa	Log - normal distribution	23.5	480
Operating pressure P_w/MPa	Gumbel maximum	0.65	7.5
Defect initial length L_i /mm	Log - normal distribution	57.65	95.2
Pipeline diameter <i>D</i> /mm	Normal distribution	120.2	620
Ultimate tensile strength v/MPa	Log - normal distribution	74.67	524
Pipeline wall thickness <i>t</i> /mm	Normal distribution	0.35	7.3

B. Prediction of pipeline failure risk level based on improved BPNN

The purpose of predicting the risk level of pipeline failure is to quantify the comprehensive impact of multidimensional parameters such as corrosion defects and pipe performance, classify pipeline risk levels, and provide a basis for accurately formulating maintenance strategies. BPNN can effectively correlate multi-parameter inputs with failure risk outputs through nonlinear mapping and self-learning capabilities. To achieve accurate classification of pipeline risks and reasonable division of failure risk levels, this study uses the dataset generated in the MCS to train a BPNN. 1,000 sets of data are selected from the dataset for the construction of a risk level prediction model. The structure of the failure risk prediction model based on BPNN is displayed in Figure 3.

In Figure 3, the input layer of the BPNN model includes six input feature parameters, including pipeline working pressure, pipe diameter, corrosion defect length, and depth. According to the empirical formula of equation (6) and through repeated experiments, the final number of hidden layers is set to 2, with 6 neurons per layer.

$$H_h = 2\sqrt{H_i + H_0} \tag{6}$$

In equation (6), H_0 and H_i are the number of output parameters and input parameters. H_h is the number of neurons in the hidden layer. The output features are the four failure risk levels of the pipeline. Each hidden layer and output layer establishes weight connections with all nodes of the previous layer, thereby achieving efficient integration and nonlinear mapping of cross-layer features. When constructing the network structure, the middle layer neurons use the Sigmoid function to provide a stable gradient backpropagation path for the feedforward signal processing mechanism. The output layer is configured with a Purelin linear activation function to ensure that the final output of the network is not constrained by the amplitude of nonlinear transformations [18]. Due to the use of gradient descent for training in traditional BPNN, it is susceptible to the influence of thresholds and weights generated by random initialization, resulting in the algorithm falling into local optima and poor generalization [19]. To address this issue, this study introduces an optimized PSO algorithm to improve BPNN. The search process of the optimized PSO is shown in Figure 4.

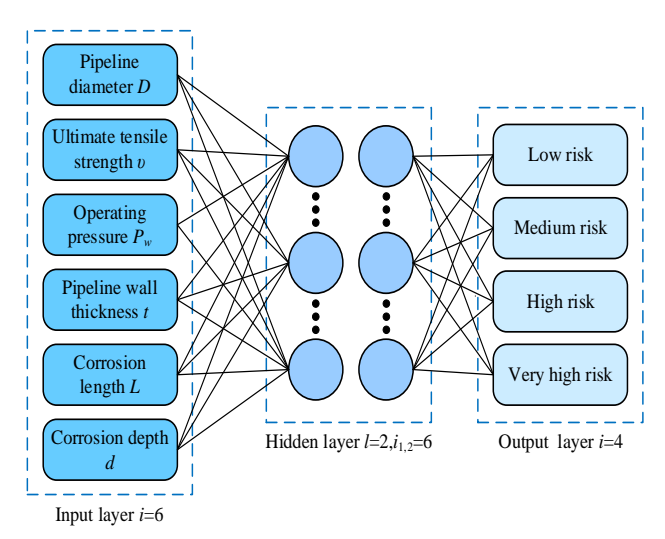


Figure 3 Structure of failure risk prediction model based on BPNN

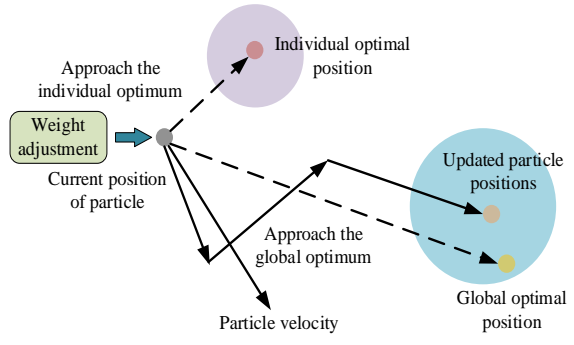


Figure 4 Search process of PSO algorithm

In Figure 4, in the optimized PSO algorithm, non-linear decreasing weights are used instead of the traditional linear decreasing strategy, as shown in equation (7).

$$w = \begin{cases} w_{\text{max}} - \frac{I \times (w_{\text{max}} - w_{\text{min}})}{I_{\text{max}}} \\ w_{\text{max}} - (w_{\text{max}} - w_{\text{min}}) \times (\frac{I}{I_{\text{max}}})^2 \end{cases}$$
 (7)

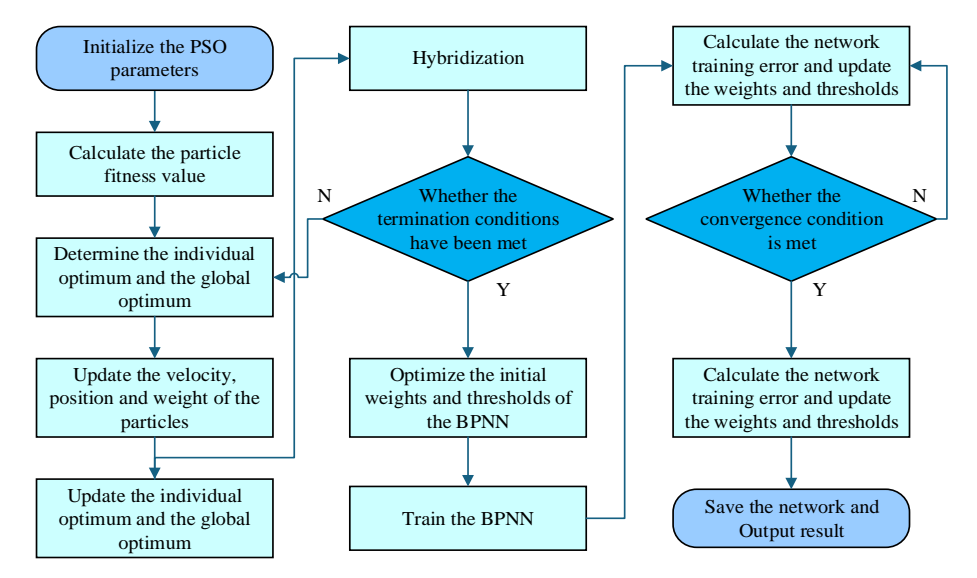


Figure 5 Flow of BPNN algorithm improved by PSO algorithm

In equation (7), I and I_{max} represent the current and maximum iteration counts. $_{w}$ is the inertia weight. w_{max} and w_{\min} are their minimum and maximum values. In this strategy, a dynamic inertia weight adjustment strategy is adopted to achieve multi-stage search optimization. In the initial stage, particles are given higher velocity vectors, allowing them to quickly traverse potential optimal regions during the global exploration phase of the solution space. As the Number of Iterations (NoI) increases, the inertia weight is dynamically adjusted through a nonlinear decay function, guiding the particle swarm to gradually enter the local search stage, where the search range exponentially shrinks to the neighborhood of the current optimal solution. When the preset maximum NoI is reached, the particle swarm mainly relies on individual cognition and social cognition components in the velocity update equation, and searches within the optimal solution neighborhood with the minimum inertia weight. In addition, to ensure the diversity of the population in the later stage of the algorithm, this study introduces the crossover operator in the algorithm, as shown in equation (8) [20].

$$sx = (1-a) * gx(2) + a * gx(1)$$
 (8)

In equation (8), a is a random number, $a \in [0,1]$. sx and gx are the positions of the child and parent particles. The speed of offspring is shown in equation (9).

$$sv = \frac{(gv(1) + gv(2)) | gv|}{|gv(1) + gv(2)|}$$
(9)

In equation (9), sv and gv are the positions of the child particles and the parent particles. At each iteration, particles select from the current population based on the crossover probability to construct a matching pool. Two particles are randomly paired to generate an equal quantum particle set. This offspring particle replaces the parent individuals with lower fitness through non-dominated sorting, thereby enhancing population diversity [21]. The improved BPNN algorithm flow of PSO is shown in Figure 5.

In Figure 5, after determining the structure of BPNN, the particle swarm parameters are initialized. The position of each particle is decoded into the weight and threshold of the neural network, and then input into the training dataset to calculate the prediction error as the fitness value of the particle. The historical optimal position of each particle and the optimal position of the current population are recorded, and the inertia weight is updated according to a nonlinear decreasing strategy. In the initial stage, it is necessary to maintain a large value to enhance global search capability, and gradually reduce it in the later stage to refine local search. Combining individual optimality, global optimality, and dynamic weights, the velocity and position of particles are updated according to PSO rules. The crossover operator of the genetic algorithm is introduced to randomly select particles for pairing, generate offspring particles to enhance population diversity, and replace low fitness parents with non-dominated sorting. If the maximum NoI is reached, the globally optimal weight and threshold will be output. Otherwise, it will return to step 2 to continue iterative optimization. The optimized weights and thresholds are loaded into BPNN to complete model training and ultimately used for predicting pipeline failure risk levels.

IV. RESULTS

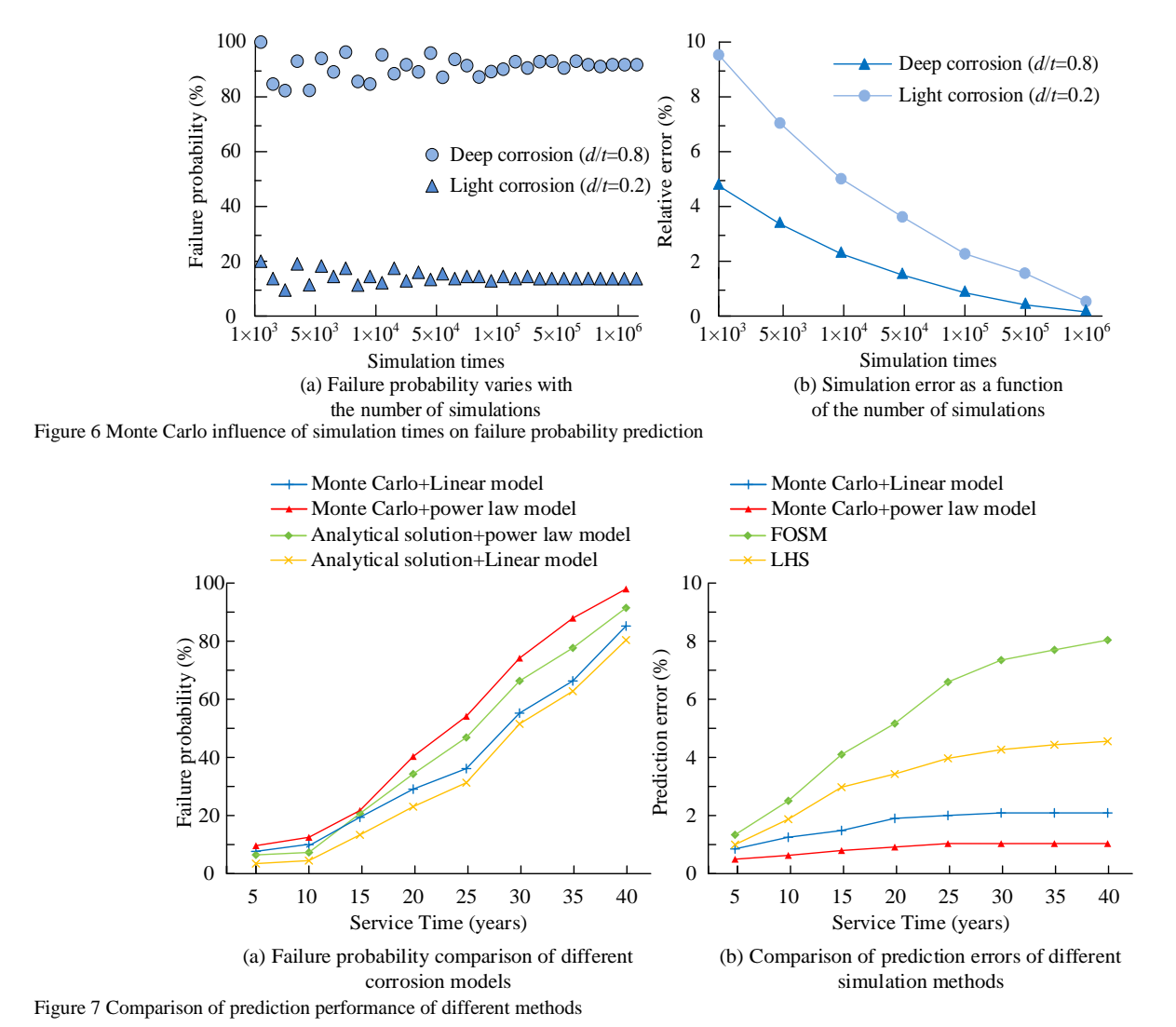
A. Analysis of the effect of Monte Carlo method

To verify the accuracy and convergence of the Monte Carlo method in predicting the failure probability of ACCPN, this study is based on the F101 model and sets the corrosion depth ratio d/t to two typical operating conditions of 0.2 and 0.8. Meanwhile, the performance of Monte Carlo is compared with Latin Hypercube Sampling (LHS) and First-Order Second Moment method (FOSM) in different performance dimensions. The experimental parameters cover typical engineering values such as a pipe diameter of 500mm and a wall thickness of 8mm. Figure 6 shows the impact of MCS iterations on failure probability prediction. Figures 6 (a) and (b) show the variation of failure probability and simulation error with the number of simulations.

In Figure 6 (a), as the number of MCSs increases from 10^3 to 10^6 , the failure probabilities at different corrosion

depths show a convergence characteristic of fluctuating first and then gradually stabilizing. Among them, the failure probability fluctuation range of deep corrosion defects with d/t=0.8 reaches 9% at low frequency (10^3 times), while it stabilizes at 93.81%±0.5% after increasing the simulation frequency to 10^5 times. The shallow corrosion defect with d/t=0.2 has less random interference and converges to 13.32% after 10^5 simulations, indicating that the deeper the corrosion depth, the higher the number of simulations required for convergence. In Figure 6 (b), the absolute error of MCS significantly decreases with increasing simulation

times. When the number of simulations increases from 10^3 to 10^6 , the absolute error of deep corrosion defects decreases from 9.52% to 0.47% at d/t=0.8, and from 4.83% to 0.14% at d/t=0.2. This indicates that the Monte Carlo method can compress errors to within ± 0.5 % through 10^6 simulations, making it suitable for high-reliability evaluation of deeply corroded pipelines. Figure 7 compares the predictive performance of different methods. Figure 7 (a) compares the failure probabilities of different corrosion models, and Figure 7 (b) compares the prediction errors of different simulation methods.



 $TABLE\ 2$ Monte Carlo verification of the comprehensive advantages of the method in F101 model

Comparison Dimension	Monte Carlo Method	Traditional Methods (LHS/FOSM)	Experimental/Reference Value
Parameter Sensitivity	<i>d/t</i> =0.6, D=500mm, t=8mm Failure Probability: 65.4%±0.5%	LHS: 65.4%±3.2% FOSM: 68.1%±7.5%	Experimental: 64.9%±1.5%
Distribution Robustness	Corrosion Depth (Log-Normal) Failure Probability: 65.4%±0.5% Corrosion Depth (Uniform) Failure Probability: 65.1%±0.6%	LHS (Uniform): 65.1%±3.1% FOSM (Fixed Mean): 67.9%±7.2%	Theoretical: 65.2%
Computational Efficiency	10^5 simulations: 120s Error: ±0.5%	LHS (10^4 simulations): 60s, ±3.2% FOSM (Analytical): 5s, ±7.5%	/
Model Adaptability	Power-Law Corrosion (α =0.78) Failure Probability: 98.1%±0.5% Linear Model (k =0.05) Failure Probability: 85.3%±2.1%	LHS (Power-Law): 98.1%±3.7% FOSM (Power-Law): 92.4%±8.3%	Experimental: 97.6%±1.8%

In Figure 7 (a), the failure prediction probability based on the Monte Carlo method combined with the power-law model is 98.1% at 40 years of service, significantly higher than the linear model and two analytical solutions. Its nonlinear growth trend accurately captures the acceleration effect of corrosion depth, while the analytical solution suffers from systematic bias due to neglecting parameter distribution. The linear model assumes a constant corrosion rate, and the long-term prediction error accumulates to 5.2%. In Figure 7 (b), the absolute error of the Monte Carlo+power-law model remains below 0.5% and does not increase with service time, while the FOSM error increases from 2.5% to 8.3% over 40 years due to the failure of linearization assumptions. This validates the advantages of Monte Carlo in nonlinear and high-dimensional parameter scenarios. Table 2 presents the comprehensive advantage verification results of the Monte Carlo method in the F101 model.

In Table 2, the Monte Carlo method demonstrates multidimensional advantages in the F101 model. The sensitivity analysis of its parameters shows that its prediction error ($\pm 0.5\%$) is reduced by more than 85% compared to traditional methods, LHS ($\pm 3.2\%$) and FOSM ($\pm 7.5\%$), and is highly consistent with experimental data ($64.9\%\pm1.5\%$). In terms of distribution robustness, the difference in failure probability under different parameter

distribution assumptions is only 0.3%, proving its insensitivity to input distribution. In terms of computational efficiency, Monte Carlo completes 10^5 simulations in 120 seconds and achieves an error of $\pm 0.5\%$, balancing speed and reliability requirements. In terms of model adaptability, the prediction error of Monte Carlo combined with a nonlinear power-law model ($\pm 0.5\%$) is reduced by 94% compared to FOSM ($\pm 8.3\%$), which verifies its ability to handle complex dynamic corrosion scenarios.

B. Performance analysis of improved BPNN

BPNN can effectively correlate multi-parameter inputs with failure risk level outputs through nonlinear mapping and self-learning capabilities. To verify the performance of the improved BPNN model in pipeline failure risk classification, this study compares the performance of traditional BPNN, Extratrees, and Random Forest based on 1,000 sets of data generated by Monte Carlo (training set: test set=8:2). The maximum NoI is 400 rounds. PSO adopts a nonlinear inertia weight $(0.9\rightarrow0.4)$ and a genetic crossover operator (crossover probability 0.7). Figure 8 shows the performance of different algorithms in the training set. Figures 8 (a) and (b) show the variation curves of precision and recall of each algorithm with the NoI.

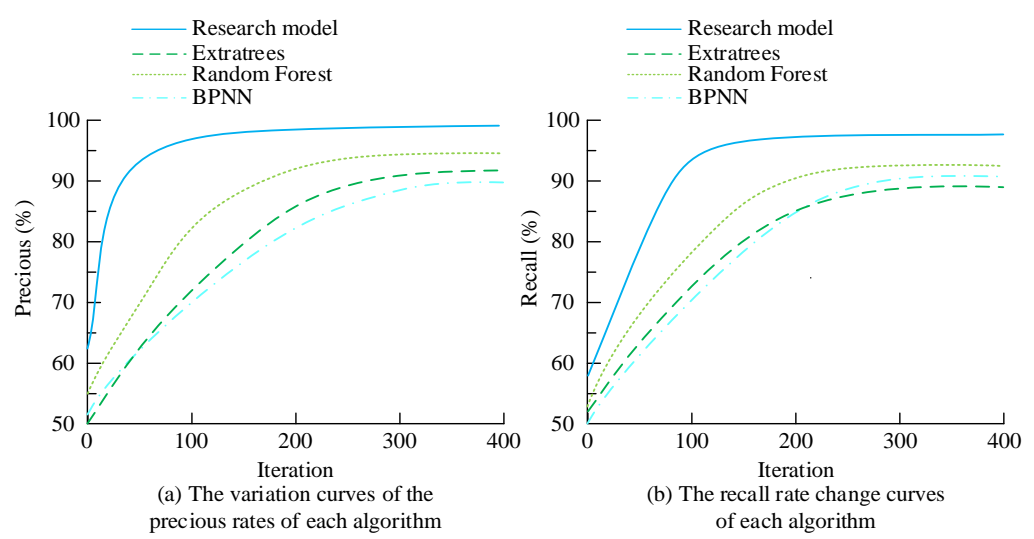


Figure 8 Variation curve of precision and recall rate of different algorithms in the training set

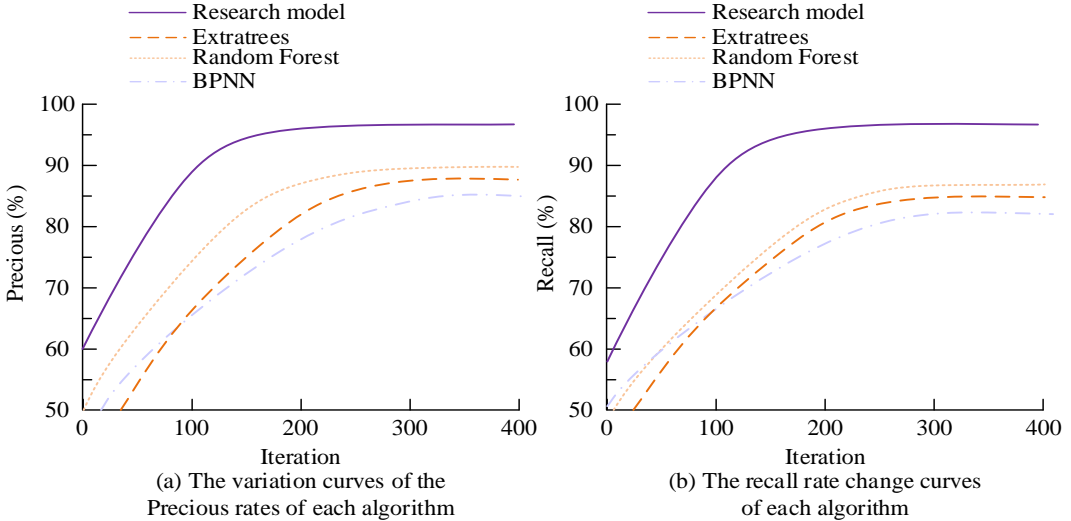
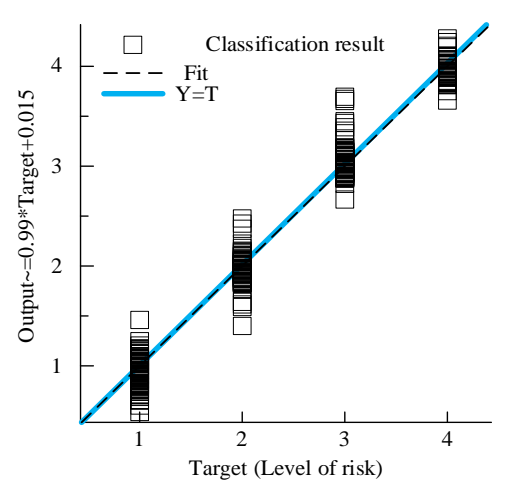
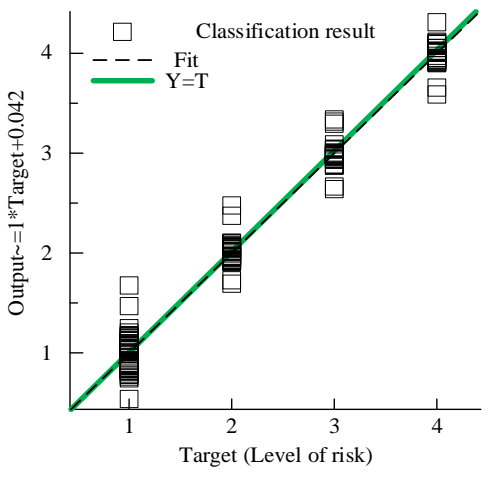


Figure 9 Variation curve of precision and recall rate of different algorithms in the test set





(a) Regression analysis of the training set results

(a) Regression analysis of the tset set results

Figure 10 Regression analysis of classification results

TABLE 3
FAILURE PROBABILITY PREDICTION RESULTS UNDER MULTI-PARAMETER COUPLING

Corrosion	Ambient	Soil resistivity	Failure probability	Error of	Relative	Experimental
growth rate α	temperature T/°C	$\rho/\Omega \cdot m$	(MC-PSO-BPNN)	traditional BPNN	improvement rate	verification value
0.6	25	10	58.2%±0.3%	8.70%	15.00%	57.9%±1.2%
0.6	35	5	$65.4\% \pm 0.4\%$	9.30%	14.20%	$64.8\% \pm 1.5\%$
0.8	25	5	$89.7\% \pm 0.2\%$	12.10%	13.50%	89.2%±1.0%
0.8	35	10	94.5%+0.3%	13.60%	14.40%	94.1%+1.3%

In Figure 8 (a), in the training set, the precision of the research method rapidly increases with the increase of iteration times and stabilizes at over 98.5% after the 100th round, significantly higher than other methods. This indicates that the nonlinear weight optimization strategy effectively improves the model's ability to recognize positive class samples. Figure 8 (b) shows that the improved model converges to 97.5% after the 150th round, which is 2.4% to 5.7% higher than traditional BPNN (convergence value of 90.9%), Extratrees (convergence value of 89.0%), and Random Forest (convergence value of 92.3%). This indicates that it can more comprehensively capture actual failure risk samples and avoid missed detections. Figures 9 (a) and (b) show the variation of precision and recall rates of four algorithms in the test set with the NoI.

In Figure 9 (a), in the test set, the precision of the research method remains at 97.2% after 200 iterations, while the precision of traditional BPNN, Extratrees, and Random Forest decreases to 85.0%, 87.7%, and 89.9%. This indicates that the PSO algorithm enhances the model's generalization ability and reduces overfitting through dynamic weight adjustment and crossover operators. Figure 9 (b) further shows that the recall rate of the research method on the test set is 97.1%, a decrease of only 0.4% compared to the training set, which is much smaller than the other three methods, verifying its stability under different data distributions. The regression analysis of the classification results of the research method in the training and testing sets is shown in Figure 10.

In Figure 10 (a), in the training set, the predicted risk level of pipeline failure by the research method is highly consistent with the actual risk level, and the slope of the fitted line is close to 1 (Output=0.99*Target+0.015), with a correlation coefficient of R=0.994. This indicates that the model can accurately map the nonlinear relationship between input parameters and risk levels, with a mean square error of 0.017 in the range of low risk (Level 1) to extremely high risk (Level 4), verifying its strong fitting

ability during the training phase. In Figure 10 (b), in the test set, the fitting equation between the predicted results of the research method and the true Output=1×Target+0.042. The data points are densely distributed near the diagonal, and the R value remains above 0.991 (R=0.991).Therefore, the research method significantly improves the accuracy and stability of risk level prediction through dynamic weight optimization and crossover operator enhancement, with a tight error distribution and no systematic bias.

To validate the proposed model's adaptability to complex multi-parameter coupled scenarios, this study employs a controlled variable method to design three representative operating conditions: corrosion growth rates $\alpha = 0.6$ (moderate corrosion rate) and $\alpha = 0.8$ (high corrosion rate), ambient temperatures $T = 25\,^{\circ}\mathrm{C}$ (ambient temperature) and $T = 35\,^{\circ}\mathrm{C}$ (high-temperature), and soil resistivity $\rho = 5\Omega\,^{\circ}\mathrm{m}$ (high-corrosive environment) and $\rho = 10\Omega\,^{\circ}\mathrm{m}$ (moderately corrosive environment). Through a full-factorial design, multi-parameter coupled scenarios are constructed. The model predictions are compared with field experimental verification values (based on three-year corrosion monitoring data from X70 steel pipelines at a northeastern oilfield). The results are presented in Table 3.

In Table 3, the prediction error of the MC-PSO-BPNN model under multi-parameter coupling conditions remains below $\pm 0.4\%$, and the maximum deviation from experimental verification values is only 0.6%, which is not affected by parameter combinations. In contrast, traditional BPNN models are unable to capture the nonlinear interactions between parameters. As the corrosion rate and environmental corrosiveness increase, the error will significantly increase (up to 13.6%). The proposed model demonstrates a stable relative improvement rate of 13.5%-15.0%, effectively validating its high precision and strong adaptability in complex operating conditions. Particularly in extreme scenarios with α =0.8 (high corrosion rate), T=35°°C (high temperature), and ρ =10° Ω ·m

(moderate corrosivity), the model accurately captures accelerated corrosion effects with 99.6% agreement with experimental values. This model further demonstrates the critical importance of multi-parameter coupling analysis in enhancing result significance.

To further validate the advantages of the proposed framework, this study conducts a systematic comparative analysis by selecting representative advanced methodologies from recent literature (References [9], [10], and [12]). All methods are executed using the same dataset generated through MCS for identical tasks, with each method employing either its original literature-reported optimal parameter configurations or default recommended settings. The comparative results are presented in Table 4.

TABLE 4
PERFORMANCE COMPARISON WITH STATE-OF-THE-ART METHODS

Method	Precision (%)	Recall (%)	F1-Score (%)	Accuracy (%)
MC-PSO-BPNN (This study)	97.2	97.1	97.15	97.3
IWOA-BPNN [9]	92.5	91.8	92.15	92.7
BES-BPNN [10]	90.0	89.5	89.75	90.2
TSO-BPNN [12]	93.8	92.7	93.25	93.5

As shown in Table 4, the research method outperformed the comparison model with 97.3% accuracy. Its precision (97.2%) and recall rate (97.1%) increased by 4.4 percentage points compared to the second-best TSO-BPNN model, while the F1 score (97.15%) further demonstrated balanced performance advantages. This validates the effectiveness of the integrated Monte Carlo data generation and improved PSO optimization mechanism. On one hand, the power-law model-based MC simulation generated high-fidelity datasets that accurately captured the nonlinear time-varying characteristics of corrosion depth. On the other hand, the PSO algorithm incorporating dynamic inertia weights and genetic crossover operators significantly enhanced BPNN's weight search efficiency through a dual-phase optimization strategy combining initial global exploration with subsequent local fine-tuning. This approach effectively overcame the common limitation of traditional intelligent algorithms like whale/owl/schoolfish optimization, which are prone to getting trapped in local optima. The results of the robustness test and computational efficiency comparison of each method for noisy data are shown in Table 5.

Table 5 presents a comprehensive comparison of the models' performance in noise resistance and computational efficiency. In terms of noise resistance, MC-PSO-BPNN achieves an accuracy rate of 95.6% under 5% Gaussian noise and maintains 92.3% accuracy even at 10% noise levels, outperforming IWOA-BPNN by 6.7% and 8.8%. This superiority over BES-BPNN and TSO-BPNN stems from the high-fidelity dataset generated through Monte Carlo methods and the enhanced robustness of the improved PSO model. Regarding efficiency, the model trained on 1,000 datasets requires only 38.6 s, representing a 31.9% reduction compared to the slowest BES-BPNN. With a single prediction time of 0.72 ms and memory consumption of 128 MB, it significantly outperforms all comparison models. Balancing precision with real-time engineering requirements, this framework demonstrates practical value data environments. complex To verify MC-PSO-BPNN framework's advantages in risk prediction accuracy, cost-effectiveness, and timeliness for practical engineering applications, this study selects 72 corrosion defect points on the X70 steel gathering pipeline network (total length 82 km) at a northeastern China oilfield as experimental subjects. Input parameters are obtained through high-precision ultrasonic thickness gauges for corrosion depth ratio measurement and pressure sensors for operational pressure recording. Pipeline age is verified against construction records, with calibration based on a comprehensive analysis of actual leakage and maintenance records from the past three years. Three senior engineers independently evaluate the benchmark using identical parameters and grading standards. The experimental process double-blind testing (separating undergoes predictions from human evaluations), with time data averaged over 10 replicates on Intel Xeon/RTX 6000 platforms. Comprehensive performance and benefit analyses of the engineering case validation are presented in Table 6.

TABLE 5

EVALUATION OF MODEL NOISE RESISTANCE AND COMPUTATIONAL EFFICIENCY

Extraction of More More Merring Court authorite Filleries				
Evaluation Index	MC-PSO-BPNN	IWOA-BPNN	BES-BPNN	TSO-BPNN
Accuracy under 5% Gaussian noise	95.60%	88.90%	87.20%	90.80%
Accuracy under 10% Gaussian noise	92.30%	83.50%	81.70%	85.40%
Training time (1000 datasets)	38.6s	52.4s	56.7s	47.9s
Single prediction time	0.72ms	1.15ms	1.28ms	0.96ms

TABLE 6 COMPREHENSIVE PERFORMANCE AND BENEFIT ANALYSIS OF REAL-WORLD CASE VALIDATION

Evaluation Dimension	Specific Metric	MC-PSO-BPNN Model	Traditional Manual Assessment
	Overall Accuracy	97.2%	80.6%
	Recall Rate for High-Risk (Level 3-4)	100%	82.1%
Technical Performance	Specificity for Low-Risk (Level 1-2)	96.2%	78.6%
	F1-Score (Macro)	97.1%	79.8%
	Kappa Coefficient	0.961	0.702
	Missed Detection for Extreme-Risk (Level 4)	0/5	1/5
Decision Reliability	Misjudgments (Medium→High Risk)	2	11
	Prediction Confidence (Avg.)	92.7%	68.4%
	Emergency Repair Cost (10 ⁴ Yuan)	280	320
Economic Indicators	Planned Maintenance Cost (10 ⁴ Yuan)	98	150
	Losses from Misjudgment (10 ⁴ Yuan)	12	86
	Total Cost (10 ⁴ Yuan)	390	556
Timeliness	Single-Point Risk Assessment Time	0.8 ms	45 min
Timenness	Full Network Scan Time (82km)	18 sec	7 days

As shown in Table 6, the MC-PSO-BPNN model demonstrates stable performance in practical engineering applications. In terms of technical performance, the model achieved an overall accuracy rate of 97.2%, representing a 16.6 percentage point improvement over manual evaluation (80.6%). Notably, the recall rate for high-risk samples (Level 3-4) reached 100% (compared to manual evaluation at 82.1%), with a Kappa consistency coefficient of 0.961, indicating high reliability in classification results. Regarding decision reliability, the model accurately identified all five extremely high-risk points (with one missed by manual evaluation), while maintaining only 2 cases of misjudgment for medium-to-high risks (compared to 11 manual cases). The average prediction confidence of 92.7% significantly outperformed the manual evaluation's 68.4%. Economically, the model reduced emergency maintenance costs by 400,000 yuan and minimized production suspension losses from misjudgments by 740,000 yuan, achieving total operational cost savings of 1.66 million yuan (a 29.9% reduction). In terms of assessment efficiency, single-point evaluation took 0.8 milliseconds, while a comprehensive scan of the 82km pipeline network required merely 18 seconds. These results demonstrate the framework's practical value in risk identification accuracy, decision stability, and engineering application efficiency.

V. CONCLUSION

To improve the accuracy of ACCPN failure assessment, this study generated a multidimensional random parameter dataset through MCS and combined it with a power-law model to describe the nonlinear time-varying characteristics of corrosion depth. An improved PSO-BPNN model was designed, incorporating nonlinear inertia weights and genetic crossover operators to optimize neural network weights and enhance global search capabilities. In the experiment, the Monte Carlo method reduced the error to 0.5% after 106 iterations, which improved the precision by over 85% compared to the traditional method (LHS/FOSM). The improved PSO-BPNN model achieved a precision of 97.2% and a recall rate of 97.1% on the test set, which was 12.2% higher than the traditional BPNN (85.0% precision). The prediction error of failure probability for deep corrosion (d/t=0.8) was only 0.47%, and the correlation coefficient of risk level classification was R>0.99, which verified the high accuracy and stability of the model under complex working conditions. The proposed fusion framework significantly improved the accuracy of pipeline failure risk assessment (error≤0.5%) and classification reliability (accuracy>97%), providing data-driven decision support for preventive maintenance of corroded pipelines. The risk level classification in this study did not take into account the impact of pipeline topology on failure propagation. Future research will introduce graph neural networks to model network topology associations and enhance system-level risk assessment capabilities.

REFERENCES

[1] E. I. Pryakhin and D. A. Pribytkova, "The Influence of the Quality of Surface Preparation of Pipes for Heating Networks on Their Corrosion Resistance During Operation in Underground Conditions," *Chernye Metally*, vol. 2023, no. 11, pp. 97-102, 2023.

- [2] G. Zheng, J. Li, D. Wang, Q. Gong, H. Xiao, and W. Huang, "Research and Application of Corrosion and Scaling Prevention Strategies for Long-Distance Heating Pipe Network with Large Temperature Difference," *Cailiao Baohu*, vol. 57, no. 9, pp. 168-174, 2024
- [3] L. Xu, Z. Zhu, and T. Li, "Exhaustive review of acceleration strategies for Monte Carlo simulations in photon transit," *Journal of Innovative Optical Health Sciences*, vol. 17, no. 5, pp. 5-21, 2024.
- [4] J. Wu, Z. Y. Rao, Y. C. Shen, B. Liao, W. W. Zhang, H. D. Zou, and H. W. Ma, "Experimental Research on Ultrasonic Guided Waves Defect Classification Based on Fractional Dimension and BP Neural Network," *Jixie Qiangdu/Journal of Mechanical Strength*, vol. 46, no. 2, pp. 328-338, 2024.
- [5] B. Hou, Q. Xu, Z. Zhong, J. Han, H. Miao, and X. Du, "Seismic Reliability Evaluation of Spatially Correlated Pipeline Networks by Quasi-Monte Carlo Simulation," Structure and Infrastructure Engineering, vol. 20, no. 4, pp. 498-513, 2024.
- [6] T. Lin, W. Huang, S. W. Liu, and R. Bai, "An Investigation on the Effect of Random Pitting Corrosion on the Strength of the Subsea Pipeline Using Monte Carlo Method," *Advanced Steel Construction*, vol. 20, no. 1, pp. 93-104, 2024.
- [7] J. Zhao, J. Li, Y. Bai, W. Zhou, Y. Zhang, and J. Wei, "Research on Leakage Detection Technology of Natural Gas Pipeline Based on Modified Gaussian Plume Model and Markov Chain Monte Carlo Method," *Process Safety and Environmental Protection*, vol. 182, no. 3, pp. 314-326, 2024.
- [8] M. Proenca, A. T. Paschoalini, and D. H. S. Obata, "Prediction of the Probabilistic Water Leak Location in Underground Pipelines Using Monte Carlo Simulation," *Water Practice and Technology*, vol. 18, no. 3, pp. 522-535, 2023.
- [9] L. Wu, J. Mei, and S. Zhao, "Pipeline Damage Identification Based on an Optimized Back-Propagation Neural Network Improved by Whale Optimization Algorithm," *Applied Intelligence*, vol. 53, no. 10, pp. 12937-12954, 2023.
- [10] P. Yin, L. Xie, H. Zhang, W. Li, and W. Wang, "Modelling Wax Deposition of Diesel in Sequential Transportation of Product Oil Pipeline Using Optimized Back Propagation Neural Network," *Canadian Journal of Chemical Engineering*, vol. 102, no. 5, pp. 1764-1776, 2024.
- [11] B. Sun, W. Zheng, A. Tong, D. Di, and Z. Li, "Prediction of the Roughness Coefficient for Drainage Pipelines with Sediments Using GA-BPNN," Water Science and Technology, vol. 88, no. 4, pp. 1111-1130, 2023.
- [12] R. Xiao, G. Liu, D. Yi, B. Liu, and Q. Zhuang, "Study on Prediction Model of Liquid Holdup Based on Back Propagation Neural Network Optimized by Tuna Swarm Algorithm," *Energy Sources Part A-Recovery Utilization and Environmental Effects*, vol. 45, no. 3, pp. 8623-8641, 2023.
- [13] M. A. Moselhy, E. G. Zaki, S. A. Abd ElMaksoud, and M. A. Migahed, "Theoretical and Electrochemical Studies of Alkyl Ammonium Halide as Impactful Inhibitors for Pipelines Corrosion in Oil Well Formation Water," *Egyptian Journal of Chemistry*, vol. 66, no. 8, pp. 543-559, 2023.
- [14] J. Wan, "Fast Risk Estimation through Fourier Transform Based Multilevel Monte Carlo Simulation," *IAENG International Journal of Applied Mathematics*, vol. 54, no. 4, pp. 730-741, 2024.
- [15] Y. Qie, T. Guo, L. Zhou, and Y. Wang, "Prediction of Burst Pressure of 20 Steel Elbow with Defects Based on SVM," *China Safety Science Journal*, vol. 33, no. 2, pp. 89-95, 2023.
- [16] Y. Wang, G. Wang, F. Xie, M. Wu, Y. Zhou, F. Liu, L. Cheng, and M. Du, "Corrosion Mechanism and Research Progress of Metal Pipeline Corrosion Under Magnetic Field and SRB Conditions: A Review," *Corrosion Reviews*, vol. 42, no. 2, pp. 203-223, 2024.
- [17] C. Li, J. Zeng, and F. Yang, "Prediction of Pipeline Failure Probability with Multiple Failure Modes and Variable Correlation," *China Safety Science Journal*, vol. 34, no. 5, pp. 36-43, 2024.
- [18] J. Hao, H. Li, F. Zhang, C. Zhang, L. Mao, and D. Liu, "Risk assessment of urban waterlogging and site selection of storage tank based on MCDM - BPNN," *China Safety Science Journal*, vol. 34, no. 8, pp. 214-221, 2024.
- [19] Y. Wang, S. Liu, X. Yang, W. Zhang, J. Yang, and J. Yang, "Optimal Design of Digital Analysis Filters Based on PSO-BPNN for Aliasing Errors Cancellation in HFB DAC," *Engineering Letters*, vol. 33, no. 1, pp. 159-168, 2025.
- [20] I. P. Okokpujie and J. E. Sinebe, "An Overview of the Study of ANN-GA, ANN-PSO, ANFIS-GA, ANFIS-PSO and ANFIS-FCM Predictions Analysis on Tool Wear During Machining Process," Journal Europeen des Systemes Automatises, vol. 56, no. 2, pp. 269-280, 2023.

IAENG International Journal of Computer Science

[21] H. Y. Shang, I. A. Deitos, and L. P. Ulrich, "Numerical Approach Based on Particle Swarm Technique for Optimization of Nonlinear Buried Pipeline on Tensionless Foundation," *Proceedings of the Institution of Mechanical Engineers Part C-Journal of Mechanical Engineering Science*, vol. 238, no. 5, pp. 1655-1670, 2024.